ISSN 1028-334X, Doklady Earth Sciences, 2021, Vol. 501, Part 1, pp. 959–962. © Pleiades Publishing, Ltd., 2021.
Russian Text © The Author(s), 2021, published in Doklady Rossiiskoi Akademii Nauk. Nauki o Zemle, 2021, Vol. 500, No. 1, pp. 73–77.

GEOPHYSICS

Features of the Phase Structure of Internal Gravity Waves Generated by a Moving Source

V. V. Bulatov[a],*, Yu. V. Vladimirov[a], I. Yu. Vladimirov[b], and E. G. Morozov[b]

Presented by Academician M.V. Flint April 15, 2021

Received April 14, 2021; revised May 11, 2021; accepted May 17, 2021

Abstract—The phase structures of internal gravity waves in the ocean are investigated. Wave fields are generated by a moving source of disturbances. The main dispersion dependences determining the properties of the generated far wave fields are studied numerically. The properties of internal waves inferred from the numerical simulations of the amplitude-phase structures of the far fields of internal gravity waves generated by moving sources of disturbances are presented. The simulations were carried out for the example of the distributions of the buoyancy frequency characteristic of the North Atlantic.

Keywords: internal gravity waves, phase structure, buoyancy frequency, wave mode

DOI: 10.1134/S1028334X21090051

Internal gravity waves (IGWs) in the ocean can be induced by any perturbation of the stratified medium [13, 15, 16]. However, the strongest generators of internal waves are tides and wind. When a tidal current runs onto the underwater slope, it generates tidal IGWs, which then propagate as free waves. IGW fields near the source are described by beams or sets of modes, with the high modes rapidly decaying and the waves of the lower modes propagating further [13, 16]. Wind action on the ocean surface practically does not generate IGWs directly: it generates inertial oscillations, which, as they collapse, generate wave packets of a wide frequency range [15, 18]. Generation of IGWs by meteorological disturbances was considered in [9, 10, 18]. Typhoons and hurricanes are the strongest generators of inertial oscillations: a typhoon can move along the surface of the ocean at a speed of several meters per second, which, as a rule, is higher than the phase velocities of IGWs in the ocean [2, 7, 9, 15, 18]. A wave wake resembling a Mach cone is formed behind the typhoon. In this wake the first inertial oscillations are excited and then a wide range of internal waves [9, 10, 18]. Such waves excited in the ocean have an actual period on the order of one hour, depending on the depth of the ocean [2, 6, 7, 15]. Internal waves can also be generated by other strong disturbances in the ocean, e.g., unstable currents, fronts, or vortices [2–4, 8, 20]. Wave fields excited through this generation mechanism can also be produced by other strong perturbations that play a significant role in various mechanisms of energy transfer in the ocean [13, 15, 16]. The propagation of dispersive IGWs in the ocean has features associated with the dependence of the propagation velocity on the wavelength. The structure of wave patterns at large distances from a moving source is practically independent of its shape and is mainly determined by the dispersion law and the velocity of the source. Modern approaches to the description of linear IGWs are based on representing wave fields by Fourier integrals, analyzing their asymptotics, and constructing phase structures within the framework of the kinematic theory of dispersive waves [3, 7, 11].

This paper considers the features of the phase and amplitude structures of the far fields of IGWs, using the distributions of the buoyancy frequency characteristics of the North Atlantic water body [5, 12, 17, 19]. Taking into account the actual stratification of temperature and salinity makes it possible to depict the patterns of wave dynamics depending on the variable density of the marine environment observed during field measurements of IGWs in the World Ocean. The North Atlantic area was chosen because this part of the ocean often experiences strong winds. The western tropical Atlantic region, located along the route of major autumn hurricanes was also considered. A similar situation is observed in the northern part of the

[a] *Ishlinskii Institute for Problems in Mechanics, Russian Academy of Sciences, Moscow, 119526 Russia*
[b] *Shirshov Institute of Oceanology, Russian Academy of Sciences, Moscow, 117218 Russia*
**e-mail: internalwave@mail.ru*

Table 1. Väisälä–Brent frequencies at the characteristic depths of the seasonal thermocline of 100 m and the main thermocline of 1000 m for the regions of the North Atlantic considered

Depth, m	Western tropical Atlantic 10° N, 43° W	Northeastern tropical Atlantic 20° N, 37° W	North Atlantic 60° N, 20° W	North Atlantic 74° N, 15° E
100	8	5	2	3
1000	2	1.5	1.5	0.8

Buoyancy (Brunt–Väisälä) frequency values for the North Atlantic regions are given in cycles per hour.

Pacific Ocean and in other areas of the ocean with strong winds; therefore, there is no fundamental difference in the physical features of wave processes. Certain differences in the numerical values in the solutions are, however, possible.

The Väisälä–Brent frequency at the characteristic depths of the seasonal 100-m thermocline and the main 1000-m thermocline for the regions of the North Atlantic considered, where domestic measurements were carried out [5, 6, 12, 17, 18], is presented below in Table 1.

In the coordinate system moving with the source, the steady field of linear IGW elevations $\eta(\xi, y, z, z_0)$ excited in an inviscid, incompressible, vertically stratified medium of finite depth at $t \to \infty$ is determined by solving the problem [3, 11]

$$V^2 \frac{\partial^2}{\partial \xi^2}\left(\frac{\partial^2}{\partial \xi^2} + \frac{\partial^2}{\partial y^2} + \frac{\partial^2}{\partial z^2}\right)\eta + N^2(z)\left(\frac{\partial^2}{\partial \xi^2} + \frac{\partial^2}{\partial y^2}\right)\eta = Q(\xi, y, z, z_0), \quad (1)$$

where V is the velocity of the source, $\xi = x + Vt$, z_0 is the depth of the source, $\eta = 0,\ z = 0,\ -H$, $N^2(z) = -\frac{g}{\rho_0(z)}\frac{d\rho_0(z)}{dz}$ is the Brunt–Väisälä frequency, $\rho_0(z)$ is the density of the unperturbed medium, and function $Q(\xi, y, z, z_0)$ describes the distribution of the source density in a moving coordinate system. At large distances, real sources of IGW disturbances allow for a physically justified approximation by a certain system of point sources taken with certain weights [3, 4, 7, 20]. The solution to problem (1) describes a steady-state wave regime in the coordinate system moving with velocity V together with the source of disturbances and has the form of the sum of wave modes [3, 11]

$$\eta(\xi, y, z, z_0) = \sum_n \eta_n(\xi, y, z, z_0),$$
$$\eta_n = \frac{1}{4\pi}\int_{-\infty}^{\infty} D_n(z, z_0, \nu)\exp(i(\mu_n(\nu)\xi - \nu y))d\nu, \quad (2)$$

where the integrand $D_n(z, z_0, \nu)$ depends on the eigenfunctions and eigenvalues $\mu_n(\nu)$, which make a solution to the equation $\omega_n^2(k) = V^2\mu_n^2(\nu)$, $k^2 = \mu_n^2(\nu) + \nu^2$, where $\omega_n(k)$ is an eigenvalue of the main vertical spectral problem of the IGW [3, 15]. As was shown in [3], the contribution of the addends describing the transient regime and depending on time in explicit form at $t \to \infty$ and fixed values of $\xi = x + Vt$ is exponentially small.

The asymptotics of integrals (2) describing the field of an individual IGW mode far from sources of disturbances can be calculated by the stationary phase method. Stationary points of the phase function are determined from the solution of the equation $\mu'(\nu) = y/\xi$. The asymptotics of the stationary phase cease to work in the vicinity of the wave fronts, that is, in the case when the stationary points tend to each other and $\mu''(\nu) \to 0$. Wave fronts are defined by ν^* values such that $\mu''(\nu^*) = 0$, and the asymptotics of the wave field near each of the wave fronts can be expressed in terms of the Airy function and its derivatives [3, 11]. In the vicinity of wave fronts, stationary points tend to zero, that is, to the edge of the integration region and, at the same time, to the singularity of the integrand $D_n(z, z_0, \nu)$. In this case, the stationary phase method is inapplicable; therefore, in order to construct local asymptotics using an appropriate transformation/substitution, the original integral should be presented as a more complex reference integral. The choice of the reference integral is determined by the distribution of stationary points of the phase function and singular points of the integrand $D_n(z, z_0, \nu)$ [14].

Far from sources of disturbances, the qualitative behavior of the wave field is determined by the presence or absence of extrema of the function $\mu'(\nu)$, corresponding to the respective stationary points of the phase functions in (2) [3, 11]. Due to the peculiarities of the distribution of the buoyancy frequency in different areas of the World Ocean, the dispersion dependences and the corresponding phase functions can have several stationary points. Below, all numerical results for the second wave mode are given without loss of generality. Figure 1 shows the calculated dispersion surfaces $\mu'(\nu, V)$. Figure 2 shows the calculated lines of equal phases (solid lines) and the corresponding wave fronts (dashed lines). Figure 3 shows the calculated elevation. Numerical calculations for different wave modes show that the dispersion pattern may have from one to several extrema of the function $\mu'(\nu)$,

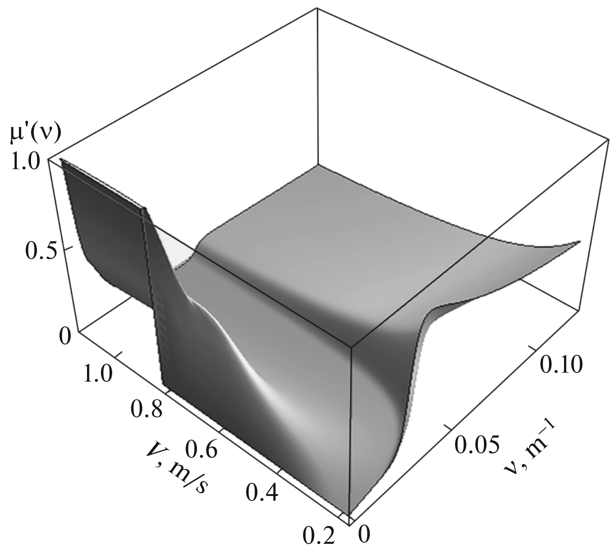

Fig. 1. Dispersion surfaces $\mu'(\nu, V)$ of internal waves.

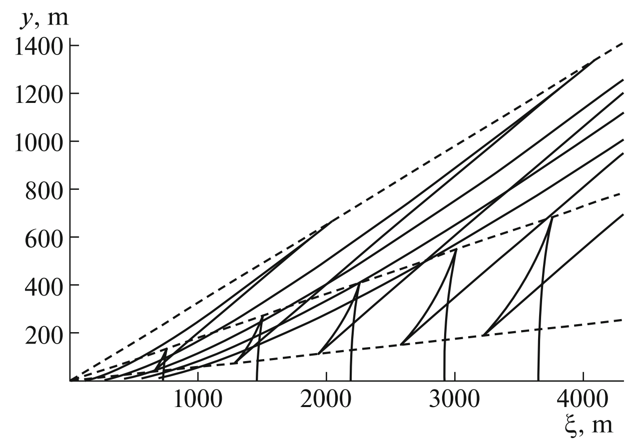

Fig. 2. Lines of equal phase during the propagation of internal waves at $V = 0.23$ m/s.

depending on distributions of the buoyancy frequency and velocity of the source. The number of extrema of the function $\mu'(\nu)$, as a rule, increases with the wave mode number, which means that several wave trains contribute to the far field of the IGW.

The results of numerical calculations show that the topology of dispersion surfaces $\mu'(\nu, V)$ can have a rather complex structure, depending both on the stratification of the medium and on the parameters of wave generation. In addition, numerical calculations show that a change in the wave generation parameters (an increase in the velocity of the source of disturbances) results in a noticeable rearrangement of the phase patterns of the wave field. In particular, the characteristic phase pattern of the "dovetail" (Fig. 2) type can be observed [1]. In this case, a qualitative restructuring of simultaneously arriving wave fronts occurs at a fixed observation point. Then the total IGW field is a complex picture of wave beats, when several wave trains with different amplitudes and phases arrive simultaneously at a certain point in space.

The complex topology of the calculated dispersion characteristics requires special mathematical methods for a correct asymptotic study of the far fields of the IGWs. Singular points of phase functions in integrals (2) can approach other singular points or the points with some peculiarity (pole, branch point) of the integrand $D_n(z, z_0, \nu)$. In this case, the standard methods for studying the asymptotics of IGW fields become inapplicable. It is important to note that the most interesting from a practical point of view are the local extrema of dispersion surfaces $\mu'(\nu, V)$, since the asymptotics of the IGW field in the vicinity of the corresponding wave fronts and caustics corresponding to these extrema can be described using the method of reference integrals. For example, when two stationary points merge, the asymptotics of integrals (2) is expressed through the Airy function, and when stationary point merge with a pole, it is expressed through the Fresnel integral. The merging of three stationary points can be described by the Pearcey function, which is often used in the theory of singularities and catastrophes [14]. If two of the three merging stationary points are strictly symmetric with respect to the third, then the asymptotics of the corresponding integral can be expressed in terms of the Hankel function. If the integrand $D_n(z, z_0, \nu)$ has a root singularity near the edge of the integration domain, then the asymptotics of the solutions are described using the square of the Airy function [3].

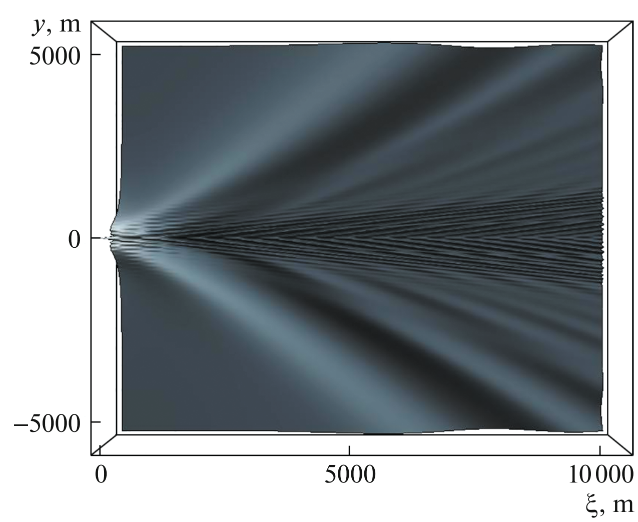

Fig. 3. Elevations during the propagation of internal waves at $V = 0.7$ m/s.

Numerical calculations of the dispersion characteristics, phase surfaces, and amplitude–phase characteristics of IGW fields show that physically interesting cases of the generation of wave structures that are not described by the well-known reference integrals can arise for actually observed vertical stratifications of the World Ocean [1, 3, 14].

FUNDING

This work was conducted in the framework of State Assignments (project nos. AAAA-A20-120011690131-7 for V.V. Bulatov and Yu.V. Vladimirov and 0128-2021-0002 for I.Yu. Vladimirov and E.G. Morozov), and supported in part by the Russian Foundation for Basic Research, project no. 20-01-00111A.

CONFLICT OF INTEREST

The authors declare that they have no conflicts of interest.

REFERENCES

1. A. I. Arnol'd, *Wave Fronts and Curves Topology* (Fazis, Moscow, 2002) [in Russian].
2. M. Yu. Belyaev, L. V. Desinov, S. K. Krikalev, S. A. Kumakshev, and S. Ya. Sekerzh-Zen'kovich, Izv. Ross. Akad. Nauk, Teor. Sist. Upr., No. 1, 117–127 (2009).
3. V. V. Bulatov and Yu. V. Vladimirov, *Waves in Stratified Medium* (Nauka, Moscow, 2015) [in Russian].
4. P. V. Matyushin, Fluid Dyn. **54** (3), 374–389 (2019).
5. E. G. Morozov, E. N. Pelinovskii, and T. G. Talipova, Oceanology **38** (4), 470–476 (1998).
6. E. G. Morozov and A. V. Marchenko, Izv., Atmos. Ocean. Phys. **48** (4), 401–409 (2012).
7. P. N. Svirkunov and M. V. Kalashnik, Usp. Fiz. Nauk **184** (1), 89 (2014).
8. A. M. Abdilghanie and P. J. Diamessis, J. Fluid Mech. **720**, 104 (2013).
9. M. H. Alford, J. A. MacKinnon, H. L. Simmons, and J. D. Nash, Annu. Rev. Mar. Sci. **8** (1), 95–123 (2016).
10. M. H. Alford, A. Y. Shcherbina, and M. C. Gregg, J. Phys. Oceanogr. **43**, 1225–1239 (2013).
11. V. V. Bulatov, Yu.V. Vladimirov, and I. Yu. Vladimirov, Russ. J. Earth Sci. **19** (5), ES5003 (2019).
12. D. I. Frey, A. N. Novigatsky, M. D. Kravchishina, and E. G. Morozov, Russ. J. Earth Sci. **17**, ES3003 (2017).
13. C. Garrett and E. Kunze, Annu. Rev. Fluid Mech. **39**, 57–87 (2007).
14. Y. Kravtsov and Y. Orlov, *Caustics, Catastrophes, and Wave Fields* (Springer, Berlin, 1999).
15. C. C. Mei, M. Stiassnie, and D. K.-P. Yue, *Theory and Applications of Ocean Surface Waves* (World Sci. Publ., London, 2017).
16. E. G. Morozov, *Oceanic Internal Tides. Observations, Analysis, and Modeling* (Springer, Dordrecht, 2018).
17. E. G. Morozov, R. Yu. Tarakanov, D. I. Frey, T. A. Demidova, and N. I. Makarenko, J. Oceanogr. **74** (2), 147–167 (2018).
18. E. G. Morozov and M. G. Velarde, J. Oceanogr. **64**, 495–509 (2008).
19. G. S. Voelker, P. G. Myers, M. Walter, and B. R. Sutherland, Dyn. Atmos. Oceans **86**, 116 (2019).
20. J. Wang, S. Wang, X. Chen, W. Wang, and Y. Xu, Phys. Fluids **29**, 106601 (2017).

Translated by M. Hannibal